https://doi.org/10.5194/tc-2019-207
Preprint. Discussion started: 6 November 2019
© Author(s) 2019. CC BY 4.0 License.

The Cryosphere Discussions

Refractory Black carbon (rBC) variability in a 47-year West Antarctic Snow and Firn core

Luciano Marquetto[1,2], Susan Kaspari[1], Jefferson Cardia Simões[2,3]

[1] Department of Geological Sciences, Central Washington University, Ellensburg, Washington ZIP Code 98926– USA
[2] Centro Polar e Climático, Universidade Federal do Rio Grande do Sul, Av, Bento Gonçalves 9500, Porto Alegre, Rio Grande do Sul CEP 91509-900 – Brazil
[3] Climate Change Institute, University of Maine, Orono, Maine 04469-5790 – USA

Correspondence to: L. Marquetto (luciano.marquetto@gmail.com)

Abstract. Black carbon (BC) is an important climate-forcing agent that affects snow albedo. In this work, we present a record of refractory black carbon (rBC) variability, measured from a 20-meter deep snow and firn core drilled in West Antarctica (79°55'34.6"S, 94°21'13.3"W) during the 2014-2015 austral summer. The core was analyzed using a Single Particle Soot Photometer (SP2) coupled to a CETAC Marin-5 nebulizer. Results show a well-defined seasonality with geometric mean concentrations of 0.015 µg L^{-1} for the wet season (summer/fall) and 0.057 µg L^{-1} for the dry season (winter/spring). The core was dated to 47 years (1968-2015) using rBC seasonality as the main parameter, along with Na, S and Sr variations. The annual rBC concentration geometric mean was 0.03 µg L^{-1}, the lowest of all rBC cores in Antarctica referenced in this work, while the annual rBC flux was 6.25 µg m^{-2} a^{-1}, the lowest flux in West Antarctica records so far. No long-term trend was observed. Snow albedo changes in the site due to BC were simulated using SNICAR-online and found to be very low comparing to clean snow (-0.48%). Fire spots inventory and BC emission estimates from the Southern Hemisphere suggest Australia and Southern Hemisphere South America as the most probable emission sources of BC to the drilling site. Spectral analysis (REDFIT method) of the BC record showed cycles related to the Antarctic Oscillation (AAO) but not to El Niño Southern Oscillation ENSO, and comparison with time series of co-registered Na record suggest BC transport to the site not to be related to the intrusion of marine air masses.

1 Introduction

Black carbon (BC) is a carbonaceous aerosol formed during incomplete combustion of biomass and fossil fuels, characterized by strong absorption of visible light and resistance to chemical transformation (Petzold et al., 2013), and plays an important role in the climatic system by being able to alter the planetary albedo (McConnell et al., 2007; Ni et al., 2014). Black carbon-containing aerosols are the species most commonly identified as being short-lived climate forcers, along with methane and ozone (AMAP, 2015). BC particles stay in the atmosphere for just one week to 10 days (Bond et al., 2013; Ni et al., 2014), but while there they change the direct radiative forcing at the top of the atmosphere by absorbing and scattering sunlight, with high spatial and temporal variability on regional scales (Bond et al., 2013). In some parts of the globe, the

https://doi.org/10.5194/tc-2019-207
Preprint. Discussion started: 6 November 2019
© Author(s) 2019. CC BY 4.0 License.


impact of BC on the climate can be even higher than greenhouse gases (Bice et al., 2009). Globally BC is estimated to be second only to CO2 in its contribution to climate forcing, with +1.1 W m^{-2} for the industrial era (1750-2005) (Bond et al., 2013; Ramanathan and Carmichael, 2008)

Increases in BC concentrations in the cryosphere since the industrial revolution have been observed, with most studies focusing on the Arctic, the Himalayas, and European glaciers as these ice caps are close to large urban centers and consequently are influenced by these. Antarctica is a pristine environment far from the rest of the world, but black carbon can still be found in its atmosphere, snow and ice, as shown by early studies (Chýlek et al., 1987, 1992; Warren and Clarke, 1990). Although there are local emissions of BC due to scientific and touristic activities (Casey et al., 2017; Stohl and Sodemann, 2010), Antarctic ice also records Southern Hemisphere (SH) emissions and long-range transport of BC from low and mid-latitudes (Bisiaux et al., 2012a, 2012b), with BC concentrations in Antarctica being linked to biomass burning from South America, Africa and Australia (Arienzo et al., 2017; Koch et al., 2007; Stohl and Sodemann, 2010). Even tropical latitude emissions have a measurable influence on the continent (Fiebig et al., 2009).

Although there are several records of SH paleo-biomass burning, there are only a few publications on BC variability in ice cores from Antarctica. Some of those are focused on centennial-millennial timescales (Arienzo et al., 2017; Chýlek et al., 1992) and others on annual to decadal scales (Bisiaux et al., 2012a, 2012b). As more ice core records are needed to understand the spatial variability of BC transport and deposition to Antarctica, as well as to improve general circulation models (Bisiaux et al., 2012b), this work aims to add another high-temporal-resolution rBC record from a West Antarctic snow and firn core to the existing literature.

2 Site Description and Field Campaign

The core (TT07) was drilled in the 2014-2015 austral summer on the Pine Island Glacier (West Antarctica) at 79°55'34.6"S, 94°21'13.3"W (elevation 2122 m above sea level – a.s.l.), near the Mount Johns Nunatak (located 70 km NE of the drilling site) (Fig. 1). We used a Mark III auger (Kovacs Enterprises, Inc.) coupled with an electrical drive powered by a generator (kept downwind at a minimum of 30 meters away) to retrieve the core. The Mark III auger recovers cylinders of 7.25cm diameter and up to one meter long. All sections of the core were weighed in the field, packed in polyethylene bags and then stored in high-density styrofoam boxes. These boxes were sent by air to Punta Arenas (Chile), then to a deposit in Bangor (ME, US) for storing and finally to the Central Washington University Ice Core Laboratory (Ellensburg, WA), where it was kept at -18°C in a clean cold room until sub-sampling and analysis.

Seasonal differences in atmospheric transport have been reported for the TT07 drilling site, with particle trajectories during the austral summer being slow moving and more locally influenced, while during the winter, air trajectories are influenced by oceanic air masses due to strong westerlies. The majority of air masses arrive from the Amundsen Sea and, secondarily, from across the Antarctic Peninsula and Weddell Sea (Schwanck et al., 2017).

https://doi.org/10.5194/tc-2019-207
Preprint. Discussion started: 6 November 2019
© Author(s) 2019. CC BY 4.0 License.


3 Methods

3.1 rBC analytical method

We used an extended range Single Particle Soot Photometer (SP2, Droplet Measurement Technologies, Boulder, CO, USA) at the Department of Geological Sciences, Central Washington University (CWU - WA, USA) to analyze our samples. The particle size range detected by the SP2 at CWU is 80-2000 nm mass-equivalent diameter for the incandescent signal, assuming a void-free black carbon density of 1.8 g cm^{-3} (Moteki and Kondo, 2010).

The SP2 measures the number and size of rBC particles using laser-induced incandescence, and was used in a variety of studies for BC in snow and ice (Bisiaux et al., 2012a, 2012b; Casey et al., 2017; Kaspari et al., 2014, 2015, 2011; McConnell et al., 2007; Osmont et al., 2018a, 2018b). In this work we use the recommended terminology by Petzold et al. (2013) and present results from the SP2 as refractory black carbon (rBC).

As the SP2 was initially designed to analyze rBC from the atmosphere (dry aerosol), a necessary step to run liquid samples is their nebulization before being coupled to the sample inlet of the SP2. For this, we used a CETAC Marin 5, described in detail by Mori et al. (2016). The authors found a good nebulizing efficiency of 50.0 ± 4.4% and no size dependency in the diameter range of 200-2000 nm. Katich et al. (2017) managed to get nebulization efficiencies near 100% with their equipment set up. We calculated the CWU Marin-5 nebulization efficiency to be 68.3 ± 5.9% (1σ) based on the external calibration carried out every working day using Aquadag standards (Marquetto et al., 2019). We found a decrease in nebulization efficiency during the laboratory work period (-0.31% per working day or -13.3% over the 43 working days), but we assume the nebulization efficiency to remain stable between the measurement of the standard and the samples measured for the day, as Katich et al. (2017). We attribute this decrease to the Marin-5 but do not see any apparent cause. Liquid pump flow rates were kept constant at 0.14 ± 0.02 mL min^{-1} during analysis.

For details of the CWU SP2 internal and external calibration, refer to Marquetto et al. (2019).

3.2 Laboratory and vial cleaning

Regular, intensive cleaning was carried out inside the cold room for all surfaces/parts/equipment in contact with the core using ethanol and laboratory-grade paper tissues. Tyvek suits (DuPont, Wilmington, DE, USA) and sterile plastic gloves were used at all times in the cold room during the core processing.

Vials used to store the samples (50 mL polypropylene vials) were soaked in Milli-Q water for 24 hours and rinsed three times. This process was repeated two more times, in a total of three days soaked in Milli-Q water and nine rinses. The vials were left to dry, covered from direct contact, in the laboratory.

3.3 Laboratory and vial cleaning

The sample preparation process consists of removing the outer layers of the core, as these are prone to contamination during drilling, handling and transport of the core (Tao et al., 2001). In the cold room, we partitioned the 21 sections of the core

https://doi.org/10.5194/tc-2019-207
Preprint. Discussion started: 6 November 2019
© Author(s) 2019. CC BY 4.0 License.


longitudinally, using a bandsaw with a meat grade, stainless steel bandsaw blade. For every cutting session, a Milli-Q (MQ) ice stick, previously prepared, was cut at the beginning, to guarantee a clean blade for the snow and firn core. After cutting the core in the bandsaw, we hand scraped the resulting snow and firn sticks with a ceramic knife in a laminar flow hood (still in the cold room) and cut them in 2 – 2.5 cm samples with the same knife (resulting in ~40 samples per section). We stored the samples in the pre-cleaned 50 mL polypropylene vials and kept them frozen until analysis.

From all steps of the sample preparation, the band saw cutting in the cold room proved to be the most prone to contaminate samples. An intensive decontamination process was carried out during a month, before we could start working with the core itself. In order to reach acceptable background levels for this step (around 0.02 µg L^{-1}), we replaced and modified some components of the band saw. We replaced the rubber tires for urethane ones; the carbon blade for a meat grade, stainless steel blade; the original plastic blade guides for ceramic ones; manufactured an acrylic blade guard, as the original plastic guard was chipping. Before using the new blade, we burned it using a blowtorch and map/pro gas (propylene with <0.5% propane) to remove any residues/oils present, then cleaned it with ethanol. For detachable parts, a detergent was used, followed by ethanol and MQ water. For parts inside the cold room, ethanol was used. We also prepared ice sticks of MQ water to cut in the band saw and help clean the blade.

3.4 Whole-system setup

The setup for the system in use at CWU is as it follows: The melted sample is dispensed to the Marin-5 nebulizer by a Reglo Digital peristaltic pump (ISMATEC, Wertheim, Germany) at 0.14 ± 0.02 mL min^{-1} and monitored by a TruFlo Sample Monitor (Glass Expansion, Port Melbourne, Australia). The Marin-5 nebulizer receives standard laboratory air at 1,000 sccm (1.000 L min^{-1}), regulated by an Alicat Flow Controller (Alicat Scientific, Tucson, AZ, USA) connected to a Drierite Gas Purifier, which removes any moisture or particulates from the air. The nebulizer heating and cooling temperatures are set to 110°C and 5°C, respectively, following (Mori et al., 2016). We used Tygon LFL tubing ID 1.02mm (Saint-Gobain Performance Plastics, France) for sample to nebulizer connection. The SP2 flow is maintained at 120 volumetric cm^3 min^{-1} (vccm). YAG laser power for this project stayed constant above 5.0 V.

Samples were analyzed for 5 minutes each. Procedural blanks (MQ water) were run at the beginning and end of every working day, and also every 15-20 samples. Background levels were kept at 0-0.5 particles cm^{-3} (translating to less than 0.01 µg L^{-1} rBC concentration), and a 5% HNO3 solution was used for cleaning the tubing and nebulizer when needed. For the SP2 to go back to background levels, only MQ water was used. Peristaltic pump tubing replacement was necessary only once during the process. The limit of detection (LOD) of the method was estimated to be 1.61x10-3 µg L^{-1} based on procedural blanks measured to characterize the instrument detection limit (mean + 3σ, n=30).

Data processing was performed with the SP2 Toolkit 4.200 developed by the Laboratory of Atmospheric Chemistry at Paul Scherer Institute (PSI), and was used on the scientific data analysis software IGOR Pro version 6.3.

https://doi.org/10.5194/tc-2019-207
Preprint. Discussion started: 6 November 2019
© Author(s) 2019. CC BY 4.0 License.


3.5 Fire spots and BC emission database

To help define the dating of the core and to investigate potential emission source regions, we compared our results with two different datasets: BC emission estimates from the Global Fire Emission Database version 4s (GFED4s - Van Der Werf et al., 2017) for the SH (SH South America, SH Africa, Australia and Equatorial Asia) and the Australian and Brazilian satellite programs, that count the fire spots (number of active fires) in Oceania and South America, respectively.

The GFED4s (https://www.globalfiredata.org/data.html) is based on the Carnegie-Ames-Stanford Approach biogeochemical model (Giglio et al., 2013), and has several improvements compared with the earlier version, including burned area and emissions from small fires as these could be substantial at a global scale (Randerson et al., 2012). BC emission estimates are given in 10^9 g and separated by region of the globe with a spatial resolution of 0.25 degree latitude by a 0.25 degree longitude. For the Southern Hemisphere, four regions are identified: Southern Hemisphere Africa (SHAF), Southern Hemisphere South America (SHSA), Australia and New Zealand (AUS) and Equatorial Asia (EQAS).

The Sentinel Hotspots (https://www.ga.gov.au/scientific-topics/earth-obs/case-studies/mapping-bushfires) and the Programa Queimadas (http://www.inpe.br/queimadas/) are fire monitoring programs run by the government of Australia (Geoscience Australia) and Brazil (Instituto Nacional de Pesquisas Espaciais - INPE), respectively. Both programs use Moderate Resolution Imaging Spectroradiometer (MODIS), Advanced Very High-Resolution Radiometer (AVHRR) and Visible Infrared Radiometer Suite (VIIRS) sensors to detect areas of elevated infrared radiation. The Sentinel Hotspots holds data from 2002 to present, while the Programa Queimadas has a record of fire spots since 1998. The parameter “fire spot” used in both Australian and Brazilian fire monitoring programs do not translate directly to the dimension and intensity of the biomass burning events, but it holds a correlation with burned area (Andela et al., 2017) and thus can be used to help date the core and investigate potential emission sources.

3.6 Core dating

Antarctic ice core rBC records from other sites show a well defined seasonality, with peak concentrations in winter-spring (dry season) due to increased biomass burning activity in the SH during this time of the year (Bisiaux et al., 2012b; Sand et al., 2017; Winstrup et al., 2017). Na and Sr also peak in the dry season (during winter) due to intense atmospheric circulation and transport (Legrand and Mayewski, 1997). Increased marine biogenic activity reflects an increase in S in late austral summer (Schwanck et al., 2017).

The core was dated by multi-parameter manual layer counting primarily driven by rBC seasonal variability, as this is a reliable parameter for dating in Antarctica (Sigl et al., 2016; Winstrup et al., 2017). We used S, Sr and Na records as additional parameters to the main counting, as these records show the more pronounced seasonal variability at the site (Schwanck et al., 2017).

Down to around 5.60 meters deep, we used the S, Sr and Na records from a core retrieved a meter apart from the rBC core during the same expedition (January 2015). Deeper than that we used the S, Sr and Na records from Schwanck et al. (2017),

https://doi.org/10.5194/tc-2019-207
Preprint. Discussion started: 6 November 2019
© Author(s) 2019. CC BY 4.0 License.


from a core drilled in the same area (less than 1 km apart) in 2008 (spanning 1883-2008), as the core collected in 2015 was not analyzed for trace elements to the full depth. Both sets of trace element samples were subsampled and analyzed at the Climate Change Institute (CCI), University of Maine (USA), so some displacement from this record to the rBC one may occur. The trace elements were analyzed by the CCI Thermo Scientific ELEMENT 2 ICP- SFMS coupled to an ESI model SC-4 autosampler; working conditions and measurement parameters are described in Schwanck et al. (2016, 2017).

We considered the new year to match the end of what we define as the dry season, as this is a reliable tie point in the record due to the abrupt drop in rBC concentrations based on the BC emission estimates from GFED4s and the fire spot databases from Australia and South America. This is also in agreement with Winstrup et al. (2017) as the authors state that BC tends to peak a little earlier than New Year in their records (Roosevelt Island Ice Core - RICE) and to Arienzo et al. (2017) as the WAIS Divide ice core presents rBC peaks in September. Also, the Pinatubo and Cerro Hudson eruptions (1991) identified in the record by Schwanck et al. (2016) and Thoen et al. (2018) were used as an absolute time horizon.

3.7 Snow accumulation, rBC concentrations and fluxes

To account for imperfections in the core geometry (and consequently imprecise density measurements), we averaged the core's density profile with the density profile from Schwanck et al. (2016) for a 45 m deep core drilled in the same region of West Antarctica. We then fitted a quadratic trend line in the average curve and used this trend line instead of the field measurements to calculate the annual snow accumulation, water equivalent (weq) and rBC fluxes. rBC fluxes were calculated by multiplying annual rBC means by annual snow accumulation.

We consider that the frequency distributions of the core rBC concentrations are lognormal, and so we present geometric means and geometric standard deviations as these are more appropriate than arithmetic calculations (Bisiaux et al., 2012a; Limpert et al., 2001). The geometric standard deviation is the multiplicative standard deviation (σ*), so the 68.3% interval of confidence is calculated as $_{\sigma}min_{conc}$ = geometric mean • geometric standard deviation, and $_{\sigma}max_{conc}$ = geometric mean/geometric standard deviation (Limpert et al., 2001). Also, correlation analysis was carried out using Mann-Kendall's test; we choose it as opposed to Spearman's test as confidence intervals are more reliable in the former (Kendall and Gibbons, 1990; Newson, 2002).

We present our data as summer/fall (dry season) concentrations and winter/spring (wet season) concentrations. Wet/dry season concentrations and annual concentration geometric means and standard deviations were calculated in the raw rBC measurements using the dating carried out to separate years and rBC concentration variations to pinpoint the changes from dry season to wet season and vice-versa. Monthly mean concentrations were calculated by applying a linear interpolation in the raw measurements, resampling the dataset to 12 values per year.

3.8 rBC impact on snow albedo

To investigate BC impact on snow albedo we used the Snow, Ice, and Aerosol Radiation (SNICAR) online model (Flanner et al., 2007). We ran the model using the parameters presented in Table 1 with varying rBC concentrations: We used the wet

https://doi.org/10.5194/tc-2019-207
Preprint. Discussion started: 6 November 2019
© Author(s) 2019. CC BY 4.0 License.


and dry season geomeans, to analyze variations for both seasons, and the highest seasonal geomean found in the core, which occurred in the dry season. As our aim in this paper is BC, we simulated albedo changes considering only the particulate and disregarding any dust/volcanic ash influence. Snow grain size used was based on Gay et al. (2002).

3.9 Spectral analysis

In order to investigate periodic oscillations (cycles) in the TT07 core and BC atmospheric transport to the drilling site, we conducted a spectral analysis in the rBC and Na records using the REDFIT procedure described in detail in Schulz and Mudelsee (2002) in the 'Past – Paleontological Statistics' software version 3.25. The spectral analysis is motivated by the observation that the most predictable (regular) behavior of a time series is to be periodic (Ghil et al., 2002). The REDFIT method is a more advanced version of the simple Lomb periodogram, and can be used for evenly and unevenly sampled data. The model is fitted to an AR(1) red noise model, the bandwidth is the spectral resolution given as the width between the -6dB points and confidence levels of 90, 95 and 99% are presented (based on chi2) (Hammer, 2019).

We choose this approach instead of estimation techniques for evenly spaced data (such as the Multitaper method) because interpolation in the time domain inevitably cause bias and alters the estimated spectrum of a time series (Schulz and Mudelsee, 2002). This way, we used the rBC and Na raw measurements (not resampled, only dated by year and separated by dry/wet season).

We compared the rBC and Na spectra with the El Niño–Southern Oscillation (ENSO), the Antarctic Oscillation (AAO) and the Amundsen Sea Low (ASL) spectra to observe possible influence of these in the rBC variability. While ENSO and AAO are well-known climate drivers, recent studies have shown the ASL has a profound effect on the West Antarctic climate (Hosking et al., 2013, 2016; Turner et al., 2013). We also compared the core records with the GFED4s BC emission estimates and the Satellite fire spots database to look for similarities between the datasets which could suggest BC emission sources to the drilling site. Table 2 shows the dataset used for the spectral analysis.

4 Results and discussion

4.1 Dating

The core was dated to 47 years, and details are presented in Fig. 2. Comparing to Schwanck et al. (2017), our dating differs by one year more considering the record in common for both cores. We attribute this difference to the addition of the rBC record to the layer counting and to the use of different cores for rBC and trace elements (see section 3.6).

4.2 Core density and annual snow accumulation

The core density (measured in the field) ranged from 0.38 to 0.60 g cm^{-3}. Using the corrected density curve obtained from our field measurements and from Schwanck et al. (2016), we calculated that the 20.16 m length core represents 10.37 m weq m (Fig. 3).

https://doi.org/10.5194/tc-2019-207
Preprint. Discussion started: 6 November 2019
© Author(s) 2019. CC BY 4.0 License.


Average annual snow accumulation is 0.21 ± 0.04 weq m per year, and varies little throughout the record, with an exception of a peak in accumulation of 0.31 weq m in 1971. The average accumulation is similar to what Banta et al. (2008) found for the WAIS Divide ice core for the last centuries (0.20 ± 0.03 weq m $year^{-1}$, elevation 1759 m a.s.l.) and to the higher altitude cores (>1700 m a.s.l.) from Kaspari et al. (2004) (0.18 to 0.23 weq m $year^{-1}$); although the latter work also presents lower altitude cores (1200 to 1600 m a.s.l.) closer to the drilling site with accumulation rates between 0.32 and 0.42 weq m $year^{-1}$.

4.3 rBC concentrations and fluxes

In agreement with others studies (Bisiaux et al., 2012a; Sand et al., 2017; Winstrup et al., 2017) we found a well-marked seasonal rBC cycle along the core, with the same pattern of low summer/fall and high winter/spring concentrations (Fig. 4). As we collected our samples in January and the drilling was carried out from the snow surface, our core starts approximately in the 2015 New Year. The core's annual rBC geometric mean concentration was 0.030 µg L^{-1} with a minimum of 0.001 µg L^{-1} and a maximum of 0.080 µg L^{-1}. Winter/spring (dry season) concentration geometric mean was 0.057 µg L^{-1}, while summer/fall (wet season) concentration geometric mean was 0.001 µg L^{-1}. Wet season average concentrations remained constant over time, while dry season average concentrations showed more variation with peak values in 1999 but no apparent trend. The main results from TT07 rBC analysis is summarized in Table 3.

We calculated annual rBC fluxes to account for potential biases in annual rBC concentrations due to changes in snow accumulation rates. Concentrations and fluxes follow a similar pattern along the core, as can be observed in Fig. 5. This means that rBC concentration variability likely reflects variations in BC emissions, transport and deposition at the site instead of reflecting changes in snow accumulation.

4.4 Comparison with other rBC records in Antarctica

BC has been studied in Antarctic snow since the late 1980s and early 1990s (Chýlek et al., 1987, 1992; Warren and Clarke, 1990). These initial studies used filter-based methods, which could under- or overestimate BC concentrations due to some analytical artifacts (Soto-García et al., 2011; Torres et al., 2014; Wang et al., 2012). Studies using the SP2 started appearing more than two decades later, aiming at recent snow rBC concentrations (Casey et al., 2017; Khan et al., 2019), near-surface air (Khan et al., 2018), recent-past ice cores (couple centuries - Bisiaux et al., 2012a, 2012b) and the past millennia (Arienzo et al., 2017). From these, a few rBC records overlap temporally with the TT07 core presented in this work, and are presented in Table 4.

The WAIS Divide rBC record from Bisiaux et al. (2012a) is the closest from TT07 (350 km apart), with similar accumulation rates. The WAIS Divide rBC annual concentration, though, is 2.7 times higher than annual values from this study (0.08 µg L^{-1} in WAIS and 0.03 µg L^{-1} in TT07 drilling site). The authors observed a steep increase in rBC concentrations in the WAIS core from 1970 to 2001 (~0.06 µg L^{-1} to ~0.11 µg L^{-1}) and related this to an increase in fossil fuel consumption and deforestation in the SH. This increasing trend was not observed in the TT07 core, that showed fairly stable annual concentrations and fluxes through time.

https://doi.org/10.5194/tc-2019-207
Preprint. Discussion started: 6 November 2019
© Author(s) 2019. CC BY 4.0 License.


The South Pole samples (1120 km from TT07) from Casey et al. (2017) were collected in early austral summer, possibly still reflecting the SH dry season. They present even higher rBC concentrations, although the samples were collected close to the Amundsen-Scott scientific station and even the "clean air sector" can present local influence, particularly in comparison to the TT07 remote site.

Khan et al. (2018) found rBC concentrations in the same order of magnitude as Casey et al. (2017), although the Dry Valleys collection site from Khan et al. (2018) was far from local interference of scientific station activities. The cores from Bisiaux et al. (2012b) (East Antarctica) present the highest elevations from the cited bibliography, and show similar rBC fluxes comparing to TT07, although these fluxes are a result of high rBC concentrations with low accumulation rates in East Antarctica, while the TT07 fluxes are the opposite – high accumulation rates (similar to the WAIS Divide core) with low rBC concentrations.

4.5 BC impact on snow albedo

To investigate BC impact on snow albedo we used SNICAR-online to simulate three scenarios with the same parameters but varying rBC concentrations: We ran the model using the wet and dry season geomeans and the highest seasonal geomean (0.015, 0.057 and 0.105 µg L^{-1}, respectively). Results show that snow albedo reduction in the TT07 site due to BC is very low to non existent (Table 5). This was already expected considering (observed) albedo reported by Casey et al. (2017): Although significant albedo reductions have been reported in more contaminated zones near the South Pole Station, the authors found a minor to negligible reduction to albedo for the "clean sector" snow.

We note that this albedo reduction occurs only in the austral summer, as the site is located almost at 80°S.

4.6 Emission sources and influence of transport on the record

Variability in ice core records reflects variability in BC emissions, atmospheric transport and deposition (Bisiaux et al., 2012a). We compared BC emissions in the SH (GFED4s and Satellite fire spots) with the TT07 rBC record.

Some models indicate that the carbonaceous load in the Antarctic troposphere mainly originates from South American emissions (Koch et al., 2007); others recognize both South America and Australia as the main sources (Stohl and Sodemann, 2010). Although Southern Africa has the largest BC emissions in the SH, it is not considered to be a significant contributor to the aerosol load in Antarctica (Li et al., 2008; Neff and Bertler, 2015; Stohl and Sodemann, 2010). Both Australia (Bisiaux et al., 2012a) and South America (Arienzo et al., 2017) have been suggested as sources of BC to West Antarctica.

Figure 6a shows the rBC monthly average values for TT07 (1968-2014) and BC monthly-averaged BC emissions from GFED4s (1997 – 2015) for the four SH emission regions (regions defined in GFED4s, see website). rBC in the TT07 starts increasing considerably in July, peaks in October and shows high but decreasing concentrations until December. African emissions are shifted left, increasing and decreasing earlier compared with other SH emission sources and with the TT07 BC record (Kendall's tau = 0.30, p = 0.17, n = 12). Equatorial Asia BC emissions increases in August and peaks in September, not reflecting the initial rBC increase in TT07 record (Kendall's tau = 0.33, p = 0.13, n = 12). The increasing trend matches

https://doi.org/10.5194/tc-2019-207
Preprint. Discussion started: 6 November 2019
© Author(s) 2019. CC BY 4.0 License.


South American emissions, as they start rising in the same period, although peaking in September and dropping significantly after (Kendall's tau = 0.66, $p < 0.01$, $n = 12$). At last, Australia and New Zealand emit much less BC than the other three regions (Fig. 6b) but atmospheric circulation favors aerosol transport from there to West Antarctica (Li et al., 2008; Neff and Bertler, 2015). Australian and New Zealand emissions start increasing in August and peak in October, falling later than the other regions (December) (Kendall's tau = 0.85, $p < 0.01$, $n = 12$). The correlation coefficients then indicate Australia/New Zealand as the most probable source region for BC at the site for the period studied, followed by SH South America. SH Africa and Equatorial Asia present much weaker correlations, which likely indicates these two regions do not contribute substantially to the rBC flux to the TT07 site. This is consistent with previous research (Arienzo et al., 2017; Bisiaux et al., 2012a).

There is a small increase in Australian emissions earlier in the year (May) that is not observed in the TT07 rBC monthly averages. This difference could be associated with the seasonal difference in particulate transport to Antarctica in winter/summer (Hara et al., 2008; Schwanck et al., 2017; Stohl and Sodemann, 2010).

4.7 Spectral analysis

We investigated further the possible emission sources and transport influences to the site using the REDFIT spectral analysis. We compared the rBC record with ENSO, AAO and ASL indexes, and to the TT07 Na record (Fig. 7), as the latter is a sea-salt proxy modulated by atmospheric transport (Legrand and Mayewski, 1997; Sneed et al., 2011). This investigation would give information about the effect of local to regional changes in atmospheric circulation on the BC records (Bisiaux et al., 2012a).

The TT07 rBC spectrum showed significant cycles in the 6-year band (AR1 Confidence Interval > 90%) and in the 2-year band (AR1 CI ~90%). Intra annual cycles in the 0.6 and 0.5 frequencies were also observed at a 95% confidence interval. Comparing the TT07 rBC record spectrum with the GFED4s and fire spots spectra, we identified similar periodicities only in the Sentinel Hotspots (Australia) record (Fig. 7), more specifically in the 2 year band (AR1 CI ~90%), and in the 0.6 year band (AR1 CI >90%). All other spectra showed only well-marked annual periodicities and intra annual periodicities of 2 and 3 cycles per year (0.5 and 0.3-year bands, not shown). We consider some of these intra annual cycles questionable, as the high-frequency end of the spectrum is often overestimated and can present aliases, 'folded signals' of another frequency process (Mudelsee, 2010; Schulz and Mudelsee, 2002), in this case aliases of the annual cycle at the 0.5 and 0.3 year bands. Due to this, we do not consider 0.5 and 0.3-year cycles to be representative.

Sea-salt transport to Antarctica (including Na) is modulated by sea level pressure (Kaspari et al., 2005; Sneed et al., 2011) and thus ASL, ENSO and ASL should influence its variability. AAO and ENSO periodicities were identified in the Na spectra (1.2 and 0.6 -year band for AAO and only 0.8-year band for ENSO). rBC and AAO also present similar cycles (2.1 and 0.6-year bands). rBC and Na spectrum show two periodicities in common, in the 1 year and 0.6-year band, but longer cycles are different. Also, differences in rBC/Na seasonality indicate the 1 year cycle does not match in the records: Na in the site typically peaks during austral winter (Schwanck et al., 2017), while rBC peaks in October, a 2-month difference

https://doi.org/10.5194/tc-2019-207
Preprint. Discussion started: 6 November 2019
© Author(s) 2019. CC BY 4.0 License.


between them (Fig. 8). The absence of longer-than-annual cycles in common and the difference in seasonality thus suggests rBC particles are not transported to the drilling site the same way as Na, by the intrusion of marine air masses.

Using the multitaper method, Bisiaux et al. (2012a) observed the rBC periodicities for the WAIS Divide ice core and Law Dome (both dated to 1850-2001). Although WAIS is closer to the TT07 drilling site (~350 km), the TT07 core presented similarities with the Law Dome spectrum (in the 6 and 2-year bands, not shown). It is not clear to us what the relation between the two sites could be, as the TT07 site location, annual accumulation and site elevation are more related to the WAIS ice core than to Law Dome (Table 4). Arienzo et al. (2017) used the multitaper method to analyze the WAIS Divide rBC flux for the period spanning 14k-6k years BP, and found a 6.6 year cycle (AR1 CI = 95%) and a 2.3 year cycle (AR1 CI > 95%), similar to the rBC cycles found in this work; although time scales and methodology used were different. Both Arienzo et al. (2017) and Bisiaux et al. (2012a) attribute the 2.3-year cycle to an indirect effect of the Quasi-Biennial Oscillation (QBO). Although the QBO circulation spans the equator to ~30°, QBO-generated variability can affect Antarctica (Strahan et al., 2015), in which case an upper troposphere/stratospheric component may be important to BC transport to the continent.

In summary, the spectral analysis suggests Australia and New Zealand as the most probable sources of rBC to the drilling site. rBC does not seem to be transported there the same way as Na, through intrusion of marine air masses. Also, rBC seems to be related to the AAO, but not to ENSO and ASL, and similarities between rBC cycles in the TT07 site and the WAIS Divide site have been observed.

5 Conclusions

BC in Antarctica has been studied only in the recent decades, but long-range anthropogenic influences have already been observed (Bisiaux et al., 2012a; Stohl and Sodemann, 2010). Models predict a continued increase in BC emissions from source areas (Bond et al., 2013) and a continued increase in BC flux to Antarctic region, mostly to the Antarctic Peninsula and West Antarctica (Arienzo et al., 2017). Understanding the spatial variability of BC is then essential to predict the particulate's future impact in the continent.

We analyzed a 20-meter long snow/firn core from West Antarctica spanning 1969-2015 for refractory black carbon. Results show a well-defined seasonal variability in the record, with low (high) concentrations during the Southern Hemisphere wet (dry) season but no long-term trend along the 47 years of the core. Snow accumulation remained stable during this period. rBC annual concentrations were found to be the lowest in samples from the recent decades compared to other studies, while rBC annual fluxes compare with the low values found by Bisiaux et al. (2012b) for high elevation East Antarctica ice cores. SNICAR modeling indicated BC does not affect snow albedo significantly at the site, with a reduction of 0.48% and 0.41% for the highest rBC concentrations found in the core and for dry season geomean concentrations relative to clean snow, respectively. Negligible impact in albedo was observed for wet season geomean concentrations. BC emission estimates and satellite data of fire spots suggest Australia and SH South America as possible emission sources to the TT07 site. Spectral

https://doi.org/10.5194/tc-2019-207
Preprint. Discussion started: 6 November 2019
© Author(s) 2019. CC BY 4.0 License.


analysis of the rBC and Na record indicate mostly different periodicities (6.2, 2.2 and 1 year cycles for rBC and 1.2, 1 and 0.8 year cycles for Na), with exception of a 0.6 year cycle in common in both spectra. Also, seasonality of rBC and Na is different, with the former peaking in October (spring) while the latter peaks in August (winter). This suggests BC is not transported to the drilling site by the same mechanisms as sea-salt (marine air masses). While we observed influence of AAO periodicities in the rBC spectrum, ENSO and ASL influences were not detected. Also, the spectral analysis showed similarities between the TT07 rBC record and the WAIS Divide rBC record, but not for the same time span. For the present time (1968-2015), the rBC spectrum showed periodicities closer to the Law Dome site from Bisiaux et al. (2012a), although no relation between the two sites is evident.

Data availability: TT07 data is available upon request; auxiliary data can be downloaded from respective sources cited along this work.

Author Contributions: Luciano Marquetto: conceptualization, investigation (fieldwork, laboratory), formal analysis, writing – original draft; Susan Kaspari: conceptualization, formal analysis, investigation (laboratory), methodology (laboratory), resources (laboratory), supervision, validation, writing – review & editing; Jefferson Cardia Simões: Conceptualization, funding acquisition, investigation (fieldwork), project administration, resources (fieldwork), supervision, writing – review & editing.

Competing interests: The authors declare that they have no conflict of interest.

Acknowledgements: This research is part of the Brazilian Antarctic Program (PROANTAR) and was financed with funds from the Brazilian National Council for Scientific and Technological Development (CNPq) Split Fellowship Program (no. 200386/2018-2, from the CNPq projects 465680/2014-3 and 442761/2018-0, CAPES project 'INCT da Criosfera' 88887.136384/2017-00 and PROANTAR project 88887.314450/2019-00. We also thank the Centro Polar e Climático (CPC/UFRGS) and the Department of Geological Sciences (CWU) faculty and staff for the support to this work.

References

AMAP: Arctic Monitoring and Assessment Programme (AMAP) assessment 2015: Black carbon and ozone as Arctic climate forcers, VII., Oslo, Norway., 2015.

Andela, N., Morton, D. C., Giglio, L., Chen, Y., van der Werf, G. R., Kasibhatla, P. S., DeFries, R. S., Collatz, G. J., Hantson, S., Kloster, S., Bachelet, D., Forrest, M., Lasslop, G., Li, F., Mangeon, S., Melton, J. R., Yue, C. and Randerson, J. T.: A human-driven decline in global burned area, Science (80-.)., 356(6345), 1356–1362, doi:10.1126/science.aal4108, 2017.

© Author(s) 2019. CC BY 4.0 License.


Arienzo, M. M., McConnell, J. R., Murphy, L. N., Chellman, N., Das, S., Kipfstuhl, S. and Mulvaney, R.: Holocene black carbon in Antarctica paralleled Southern Hemisphere climate, J. Geophys. Res., 122(13), 6713–6728, doi:10.1002/2017JD026599, 2017.

Banta, J. R., McConnell, J. R., Frey, M. M., Bales, R. C. and Taylor, K.: Spatial and temporal variability in snow accumulation at the West Antarctic Ice Sheet Divide over recent centuries, J. Geophys. Res. Atmos., 113(23), doi:10.1029/2008JD010235, 2008.

Bice, K., Eil, A., Habib, B., Heijmans, P., Kopp, R., Nogues, J., Norcross, F., Sweizer-Hamilton, M. and Whitworth, A.: Black carbon: A review and policy recommendations, Princeton, NJ, EUA. [online] Available from: http://scholar.google.com/scholar?hl=en&btnG=Search&q=intitle:Black+Carbon:+A+Review+and+Policy+recommendations#0, 2009.

Bisiaux, M. M., Edwards, R., McConnell, J. R., Curran, M. a J., Van Ommen, T. D., Smith, a. M., Neumann, T. a., Pasteris, D. R., Penner, J. E. and Taylor, K.: Changes in black carbon deposition to Antarctica from two high-resolution ice core records, 1850-2000 AD, Atmos. Chem. Phys., 12(9), 4107–4115, doi:10.5194/acp-12-4107-2012, 2012a.

Bisiaux, M. M., Edwards, R., McConnell, J. R., Albert, M. R., Anschütz, H., Neumann, T. a., Isaksson, E. and Penner, J. E.: Variability of black carbon deposition to the East Antarctic Plateau, 1800-2000 AD, Atmos. Chem. Phys., 12(8), 3799–3808, doi:10.5194/acp-12-3799-2012, 2012b.

Bond, T. C., Doherty, S. J., Fahey, D. W., Forster, P. M., Berntsen, T., Deangelo, B. J., Flanner, M. G., Ghan, S., Kärcher, B., Koch, D., Kinne, S., Kondo, Y., Quinn, P. K., Sarofim, M. C., Schultz, M. G., Schulz, M., Venkataraman, C., Zhang, H., Zhang, S., Bellouin, N., Guttikunda, S. K., Hopke, P. K., Jacobson, M. Z., Kaiser, J. W., Klimont, Z., Lohmann, U., Schwarz, J. P., Shindell, D., Storelvmo, T., Warren, S. G. and Zender, C. S.: Bounding the role of black carbon in the climate system: A scientific assessment, J. Geophys. Res. Atmos., 118(11), 5380–5552, doi:10.1002/jgrd.50171, 2013.

Casey, K. A., Kaspari, S. D., Skiles, S. M., Kreutz, K. and Handley, M. J.: The spectral and chemical measurement of pollutants on snow near South Pole, Antarctica, J. Geophys. Res. Atmos., 122(12), 6592–6610, doi:10.1002/2016JD026418, 2017.

Chýlek, P., Srivastava, V., Cahenzli, L., Pinnick, R. G., Dod, R. L., Novakov, T., Cook, T. L. and Hinds, B. D.: Aerosol and graphitic carbon content of snow, J. Geophys. Res., 92(D8), 9801, doi:10.1029/JD092iD08p09801, 1987.

Chýlek, P., Johnson, B. and WU, H.: Black carbon concentration in Byrd Station ice core : from 13,000 to 700 years before present, Ann. Geophys., 10(8), 625–629 [online] Available from: http://cat.inist.fr/?aModele=afficheN&cpsidt=5456751 (Accessed 5 May 2016), 1992.

Fiebig, M., Lunder, C. R. and Stohl, a.: Tracing biomass burning aerosol from South America to Troll Research Station, Antarctica, Geophys. Res. Lett., 36(14), 1–5, doi:10.1029/2009GL038531, 2009.

Flanner, M. G., Zender, C. S., Randerson, J. T. and Rasch, P. J.: Present-day climate forcing and response from black carbon in snow, J. Geophys. Res. Atmos., 112(11), 1–17, doi:10.1029/2006JD008003, 2007.

Gay, M., Fily, M., Genthon, C., Frezzotti, M., Oerter, H. and Winther, J.-G.: Snow grain-size measurements in Antarctica, J. Glaciol., 48(163), 527–535, doi:10.3189/172756502781831016, 2002.

Ghil, M., Allen, M. R., Dettinger, M. D., Ide, K., Kondrashov, D., Mann, M. E., Robertson, A. W., Saunders, A., Tian, Y., Varadi, F. and Yiou, P.: Advanced spectral methods for climatic time series, Rev. Geophys., 40(1), doi:10.1029/2000RG000092, 2002.

Giglio, L., Randerson, J. T. and Van Der Werf, G. R.: Analysis of daily, monthly, and annual burned area using the fourth-generation global fire emissions database (GFED4), J. Geophys. Res. Biogeosciences, 118(1), 317–328, doi:10.1002/jgrg.20042, 2013.

Hammer, Ø.: Past - Paleontological Statistics Version 3.25 reference manual, , 1, 275, 2019.

Hara, K., Osada, K., Yabuki, M., Hayashi, M., Yamanouchi, T., Shiobara, M. and Wada, M.: Black carbon at Syowa station,

© Author(s) 2019. CC BY 4.0 License.


Antarctica Measurement of black carbon at Syowa station, Antarctica: seasonal variation, transport processes and pathways, ACPD Atmos. Chem. Phys. Discuss. Atmos. Chem. Phys. Discuss., 8(8), 9883–9929, doi:10.5194/acpd-8-9883-2008, 2008.

Hosking, J. S., Orr, A., Marshall, G. J., Turner, J. and Phillips, T.: The influence of the amundsen-bellingshausen seas low on the climate of West Antarctica and its representation in coupled climate model simulations, J. Clim., 26(17), 6633–6648, doi:10.1175/JCLI-D-12-00813.1, 2013.

Hosking, J. S., Orr, A., Bracegirdle, T. J. and Turner, J.: Future circulation changes off West Antarctica: Sensitivity of the Amundsen Sea Low to projected anthropogenic forcing, Geophys. Res. Lett., 43(1), 367–376, doi:10.1002/2015GL067143, 2016.

Kaspari, S., Mayewski, P. A., Dixon, D. A., Spikes, V. B., Sneed, S. B., Handley, M. J. and Hamilton, G. S.: Climate variability in West Antarctica derived from annual accumulation-rate records from ITASE firn/ice cores, Ann. Glaciol., 39(3), 585–594, 2004.

Kaspari, S., Painter, T. H., Gysel, M., Skiles, S. M. and Schwikowski, M.: Seasonal and elevational variations of black carbon and dust in snow and ice in the Solu-Khumbu, Nepal and estimated radiative forcings, Atmos. Chem. Phys., 14(15), 8089–8103, doi:10.5194/acp-14-8089-2014, 2014.

Kaspari, S., Skiles, S. M. K., Delaney, I., Dixon, D. and Painter, T. H.: Accelerated glacier melt on Snow Dome, Mount Olympus, Washington, USA, due to deposition of black carbon and mineral dust from wildfire, J. Geophys. Res., 120(7), 2793–2807, doi:10.1002/2014JD022676, 2015.

Kaspari, S. D., Dixon, D. a., Sneed, S. B. and Handley, M. J.: Sources and transport pathways of marine aerosol species into West Antarctica, Ann. Glaciol., 41, 1–9, doi:10.3189/172756405781813221, 2005.

Kaspari, S. D., Schwikowski, M., Gysel, M., Flanner, M. G., Kang, S., Hou, S. and Mayewski, P. a.: Recent increase in black carbon concentrations from a Mt. Everest ice core spanning 1860-2000 AD, Geophys. Res. Lett., 38(4), 11–16, doi:10.1029/2010GL046096, 2011.

Katich, J. M., Perring, A. E. and Schwarz, J. P.: Optimized detection of particulates from liquid samples in the aerosol phase: Focus on black carbon, Aerosol Sci. Technol., 51(5), 543–553, doi:10.1080/02786826.2017.1280597, 2017.

Kendall, M. and Gibbons, J. D.: Rank Correlation Methods, 5th editio., edited by E. Arnold, Oxford University Press, London., 1990.

Khan, A. L., McMeeking, G. R., Schwarz, J. P., Xian, P., Welch, K. A., Berry Lyons, W. and McKnight, D. M.: Near-Surface Refractory Black Carbon Observations in the Atmosphere and Snow in the McMurdo Dry Valleys, Antarctica, and Potential Impacts of Foehn Winds, J. Geophys. Res. Atmos., 123(5), 2877–2887, doi:10.1002/2017JD027696, 2018.

Khan, A. L., Klein, A. G., Katich, J. M. and Xian, P.: Local Emissions and Regional Wildfires Influence Refractory Black Carbon Observations Near Palmer Station, Antarctica, Front. Earth Sci., 7(April), 1–8, doi:10.3389/feart.2019.00049, 2019.

Koch, D., Bond, T. C., Streets, D., Unger, N. and van der Werf, G. R.: Global impacts of aerosols from particular source regions and sectors, J. Geophys. Res. Atmos., 112(2), 1–24, doi:10.1029/2005JD007024, 2007.

Legrand, M. and Mayewski, P.: Glaciochemistry of polar ice cores: A review, Rev. Geophys., 35(3), 219–243, doi:10.1029/96RG03527, 1997.

Li, F., Ginoux, P. and Ramaswamy, V.: Distribution, transport, and deposition of mineral dust in the Southern Ocean and Antarctica: Contribution of major sources, J. Geophys. Res. Atmos., 113(10), 1–15, doi:10.1029/2007JD009190, 2008.

Limpert, E., Stahel, W. A. and Abbt, M.: Log-normal Distributions across the Sciences: Keys and Clues, Bioscience, 51(5), 341–352, doi:10.1641/0006-3568(2001)051[0341:lndats]2.0.co;2, 2001.

Marquetto, L., Kaspari, S., Simões, J. C. and Babik, E.: Refractory Black Carbon results and a method comparison between solid-state cutting and continuous melting sampling of a West Antarctic snow and firn core, Manuscr. Submitt. Publ., 2019.

Matsuoka, K., Skoglund, A. and Roth, G.: Quantarctica [Data set], , doi:https://doi.org/10.21334/npolar.2018.8516e961,

© Author(s) 2019. CC BY 4.0 License.


2018.

McConnell, J. R., Edwards, R., Kok, G. L., Flanner, M. G., Zender, C. S., Saltzman, E. S., Banta, J. R., Pasteris, D. R., Carter, M. M. and Kahl, J. D. W.: 20th-Century Industrial Black Carbon Emissions Altered Arctic Climate Forcing, Science (80-.)., 317(September), 1381–1384, 2007.

Mori, T., Moteki, N., Ohata, S., Koike, M., Goto-Azuma, K., Miyazaki, Y. and Kondo, Y.: Improved technique for measuring the size distribution of black carbon particles in liquid water, Aerosol Sci. Technol., 50(3), 242–254, doi:10.1080/02786826.2016.1147644, 2016.

Moteki, N. and Kondo, Y.: Dependence of laser-induced incandescence on physical properties of black carbon aerosols: Measurements and theoretical interpretation, Aerosol Sci. Technol., 44(8), 663–675, doi:10.1080/02786826.2010.484450, 2010.

Mudelsee, M.: Climate Time Series Analysis, Springer Netherlands, Dordrecht., 2010.

Neff, P. D. and Bertler, N. A. N.: Trajectory modeling of modern dust transport to the Southern Ocean and Antarctica, J. Geophys. Res. Atmos., 120, 9303–9322, doi:10.1002/2015JD023304, 2015.

Newson, R.: Parameters behind "Nonparametric" Statistics: Kendall's tau, Somers' D and Median Differences, Stata J. Promot. Commun. Stat. Stata, 2(1), 45–64, doi:10.1177/1536867x0200200103, 2002.

Ni, M., Huang, J., Lu, S., Li, X., Yan, J. and Cen, K.: A review on black carbon emissions, worldwide and in China, Chemosphere, 107, 83–93, doi:10.1016/j.chemosphere.2014.02.052, 2014.

Osmont, D., Sigl, M., Eichler, A., Jenk, T. M. and Schwikowski, M.: A Holocene black carbon ice-core record of biomass burning in the Amazon Basin from Illimani, Bolivia, Clim. Past Discuss., 15, 579–592, doi:10.5194/cp-2018-136, 2018a.

Osmont, D., Wendl, I. A., Schmidely, L., Sigl, M., Vega, C. P., Isaksson, E. and Schwikowski, M.: An 800 year high-resolution black carbon ice-core record from Lomonosovfonna, Svalbard, Atmos. Chem. Phys. Discuss., 1–30, doi:10.5194/acp-2018-244, 2018b.

Petzold, a., Ogren, J. a., Fiebig, M., Laj, P., Li, S. M., Baltensperger, U., Holzer-Popp, T., Kinne, S., Pappalardo, G., Sugimoto, N., Wehrli, C., Wiedensohler, a. and Zhang, X. Y.: Recommendations for reporting black carbon measurements, Atmos. Chem. Phys., 13(16), 8365–8379, doi:10.5194/acp-13-8365-2013, 2013.

Ramanathan, V. and Carmichael, G.: Global and regional climate changes due to black carbon, Nat. Geosci., 1(4), 221–227, doi:10.1038/ngeo156, 2008.

Randerson, J. T., Chen, Y., Van Der Werf, G. R., Rogers, B. M. and Morton, D. C.: Global burned area and biomass burning emissions from small fires, J. Geophys. Res. Biogeosciences, 117(4), doi:10.1029/2012JG002128, 2012.

Sand, M., Samset, B. H., Balkanski, Y., Bauer, S., Bellouin, N., Berntsen, T. K., Bian, H., Chin, M., DIehl, T., Easter, R., Ghan, S. J., Iversen, T., Kirkeväg, A., Lamarque, J. F., Lin, G., Liu, X., Luo, G., Myhre, G., Van Noije, T., Penner, J. E., Schulz, M., Seland, O., Skeie, R. B., Stier, P., Takemura, T., Tsigaridis, K., Yu, F., Zhang, K. and Zhang, H.: Aerosols at the poles: An AeroCom Phase II multi-model evaluation, Atmos. Chem. Phys., 17(19), 12197–12218, doi:10.5194/acp-17-12197-2017, 2017.

Schulz, M. and Mudelsee, M.: REDFIT: Estimating red-noise spectra directly from unevenly spaced paleoclimatic time series, Comput. Geosci., 28(3), 421–426, doi:10.1016/S0098-3004(01)00044-9, 2002.

Schwanck, F., Simões, J. C., Handley, M., Mayewski, P. A., Bernardo, R. T. and Aquino, F. E.: Drilling, processing and first results for Mount Johns ice core in West Antarctica Ice Sheet, Brazilian J. Geol., 46(1), 29–40, doi:10.1590/2317-4889201620150035, 2016.

Schwanck, F., Simões, J. C., Handley, M., Mayewski, P. A., Auger, J. D., Bernardo, R. T. and Aquino, F. E.: A 125-year record of climate and chemistry variability at the Pine Island Glacier ice divide, Antarctica, Cryosphere, 11(4), 1537–1552, doi:10.5194/tc-11-1537-2017, 2017.

© Author(s) 2019. CC BY 4.0 License.

Sigl, M., Fudge, T. J., Winstrup, M., Cole-Dai, J., Ferris, D., McConnell, J. R., Taylor, K. C., Welten, K. C., Woodruff, T. E., Adolphi, F., Bisiaux, M., Brook, E. J., Buizert, C., Caffee, M. W., Dunbar, N. W., Edwards, R., Geng, L., Iverson, N., Koffman, B., Layman, L., Maselli, O. J., McGwire, K., Muscheler, R., Nishiizumi, K., Pasteris, D. R., Rhodes, R. H. and Sowers, T. A.: The WAIS Divide deep ice core WD2014 chronology - Part 2: Annual-layer counting (0-31 ka BP), Clim. Past, 12(3), 769–786, doi:10.5194/cp-12-769-2016, 2016.

Sneed, S. B., Mayewski, P. A. and Dixon, D. A.: An emerging technique: Multi-ice-core multi-parameter correlations with Antarctic sea-ice extent, Ann. Glaciol., 52(57 PART 2), 347–354, doi:10.3189/172756411795931822, 2011.

Soto-García, L. L., Andreae, M. O., Andreae, T. W., Artaxo, P., Maenhaut, W., Kirchstetter, T., Novakov, T., Chow, J. C. and Mayol-Bracero, O. L.: Evaluation of the carbon content of aerosols from the burning of biomass in the Brazilian Amazon using thermal, optical and thermal-optical analysis methods, Atmos. Chem. Phys., 11(9), 4425–4444, doi:10.5194/acp-11-4425-2011, 2011.

Stohl, A. and Sodemann, H.: Characteristics of atmospheric transport into the Antarctic troposphere, J. Geophys. Res. Atmos., 115(D2), 1–16, doi:10.1029/2009JD012536, 2010.

Strahan, S. E., Oman, L. D., Douglass, A. R. and Coy, L.: Modulation of Antarctic vortex composition by the quasi-biennial oscillation, Geophys. Res. Lett., 42(10), 4216–4223, doi:10.1002/2015GL063759, 2015.

Tao, G., Yamada, R., Fujikawa, Y., Kudo, A., Zheng, J., Fisher, D. A. and Koerner, R. M.: Determination of trace amounts of heavy metals in arctic ice core samples using inductively coupled plasma mass spectrometry, Talanta, 55(4), 765–772, doi:10.1016/S0039-9140(01)00509-4, 2001.

Thoen, I. U., Simões, J. C., Lindau, F. G. L. and Sneed, S. B.: Ionic content in an ice core from the West Antarctic Ice Sheet: 1882-2008 A.D., Brazilian J. Geol., 48(4), 853–865, doi:10.1590/2317-4889201820180037, 2018.

Torres, A., Bond, T. C., Lehmann, C. M. B., Subramanian, R. and Hadley, O. L.: Measuring organic carbon and black carbon in rainwater: Evaluation of methods, Aerosol Sci. Technol., 48(3), 239–250, doi:10.1080/02786826.2013.868596, 2014.

Turner, J., Phillips, T., Hosking, J. S., Marshall, G. J. and Orr, A.: The Amundsen Sea low, , 1829(August 2012), 1818–1829, doi:10.1002/joc.3558, 2013.

Wang, M., Xu, B., Zhao, H., Cao, J., Joswiak, D., Wu, G. and Lin, S.: The Influence of Dust on Quantitative Measurements of Black Carbon in Ice and Snow when Using a Thermal Optical Method, Aerosol Sci. Technol., 46(1), 60–69, doi:10.1080/02786826.2011.605815, 2012.

Warren, S. G. and Clarke, A. D.: Soot in the atmosphere and snow surface of antarctica, J. Geophys. Res., 95(D2), 1811–1816, 1990.

Van Der Werf, G. R., Randerson, J. T., Giglio, L., Van Leeuwen, T. T., Chen, Y., Rogers, B. M., Mu, M., Van Marle, M. J. E., Morton, D. C., Collatz, G. J., Yokelson, R. J. and Kasibhatla, P. S.: Global fire emissions estimates during 1997-2016, Earth Syst. Sci. Data, 9(2), 697–720, doi:10.5194/essd-9-697-2017, 2017.

Winstrup, M., Vallelonga, P., Kjær, H. A., Fudge, T. J., Lee, J. E., Riis, M. H., Edwards, R., Bertler, N. A. N., Blunier, T., Brook, E. J., Buizert, C., Ciobanu, G., Conway, H., Dahl-Jensen, D., Ellis, A., Emanuelsson, B. D., Keller, E. D., Kurbatov, A., Mayewski, P., Neff, P. D., Pyne, R., Simonsen, M. F., Svensson, A., Tuohy, A., Waddington, E. and Wheatley, S.: A 2700-year annual timescale and accumulation history for an ice core from Roosevelt Island, West Antarctica, Clim. Past Discuss., 1(August), 1–46, doi:10.5194/cp-2017-101, 2017.

https://doi.org/10.5194/tc-2019-207
Preprint. Discussion started: 6 November 2019
© Author(s) 2019. CC BY 4.0 License.

The Cryosphere Discussions
Open Access
EGU

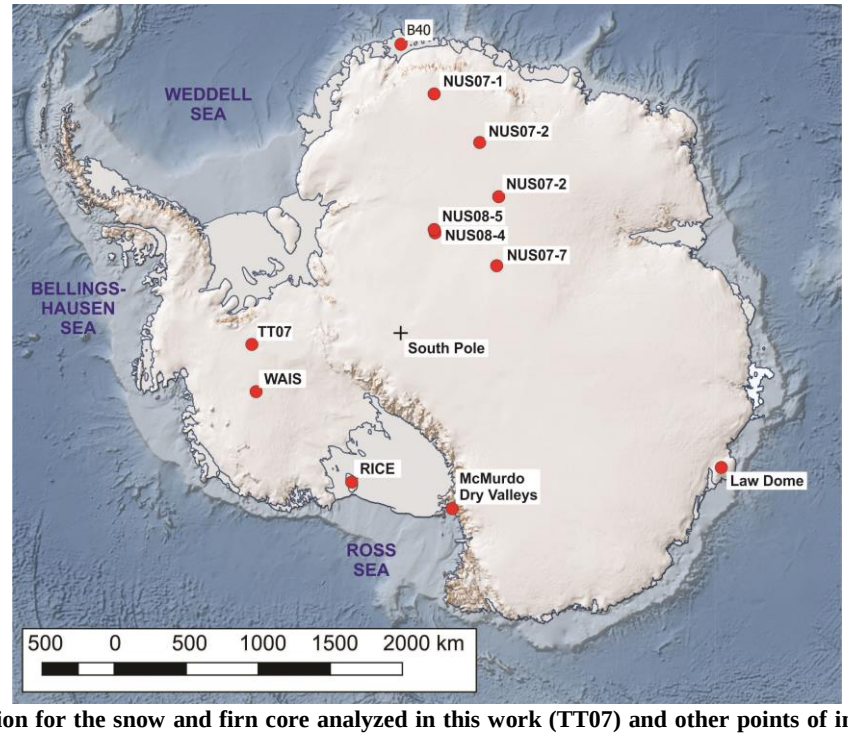

Figure 1. Drilling location for the snow and firn core analyzed in this work (TT07) and other points of interest mentioned in the text. Basemap from the Quantarctica Project (Matsuoka et al., 2018).

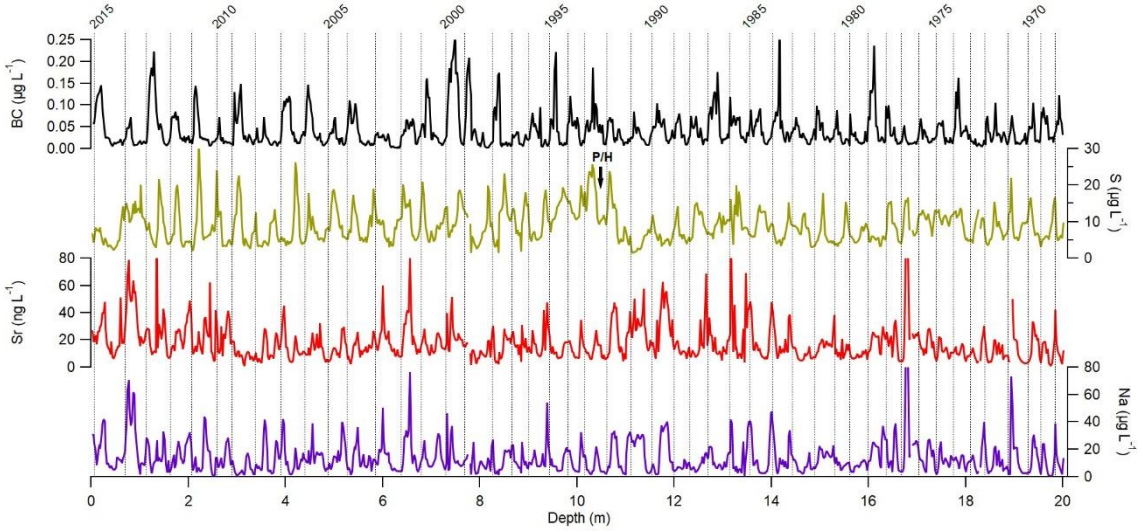

Figure 2. Dating of the snow and firn core based on rBC and using S, Sr and Na records from nearby cores (see section 3.6) as support. Dashed lines indicate estimated New Year and "P/H" in the sulphur record around 10 m indicate Pinatubo/Cerro Hudson signal identified by Schwanck et al. (2017) and Thoen et al. (2018) and used as an absolute time horizon.

https://doi.org/10.5194/tc-2019-207
Preprint. Discussion started: 6 November 2019
© Author(s) 2019. CC BY 4.0 License.

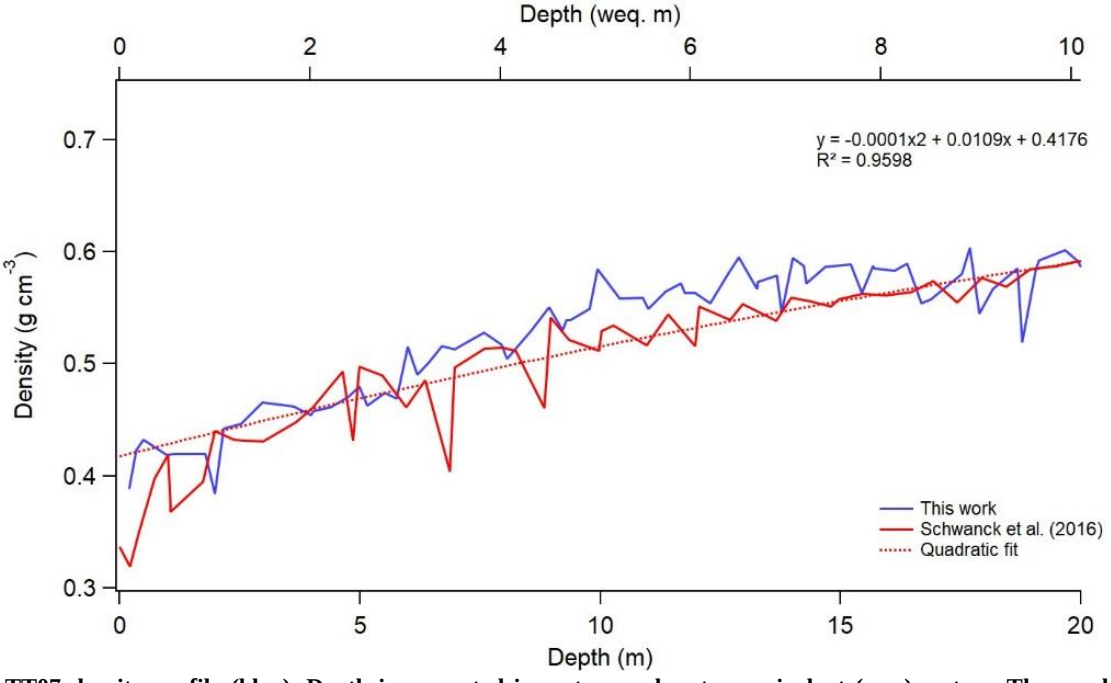

Figure 3. TT07 density profile (blue). Depth is presented in meters and water equivalent (weq) meters. The quadratic fit was calculated from the average density profile from this work and from Schwanck et al. (2016).

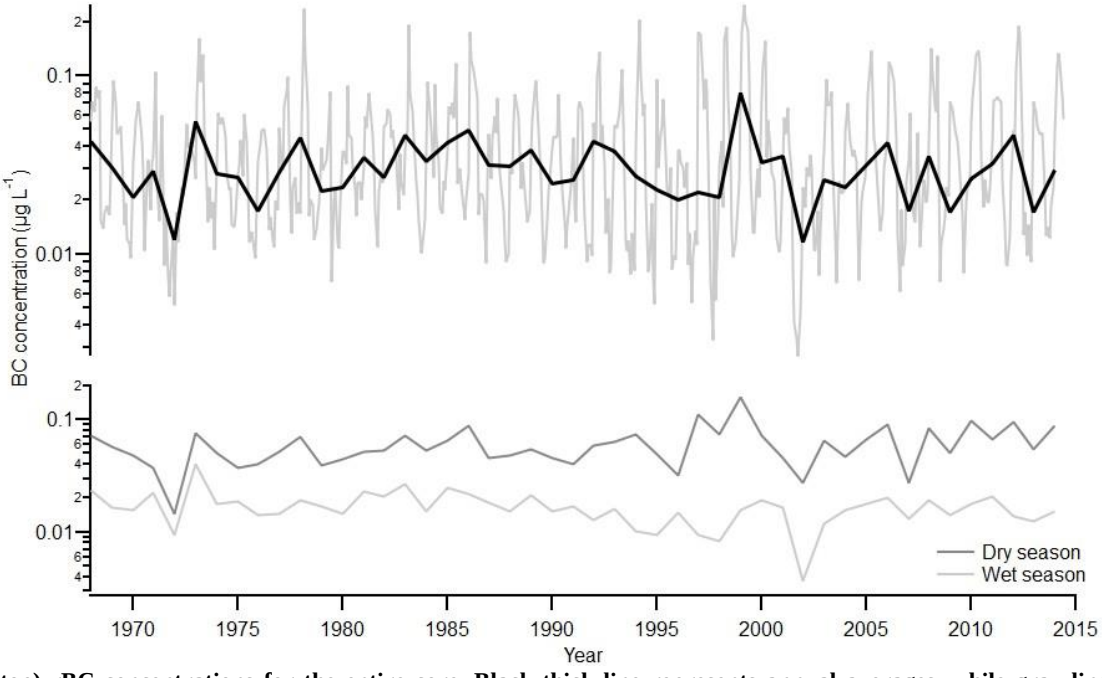

Figure 4. (top) rBC concentrations for the entire core. Black thick line represents annual averages, while gray line represents monthly values. Note the y axis scale is logarithmic. (base) Dry season and wet season average concentrations per year.

https://doi.org/10.5194/tc-2019-207
Preprint. Discussion started: 6 November 2019
© Author(s) 2019. CC BY 4.0 License.

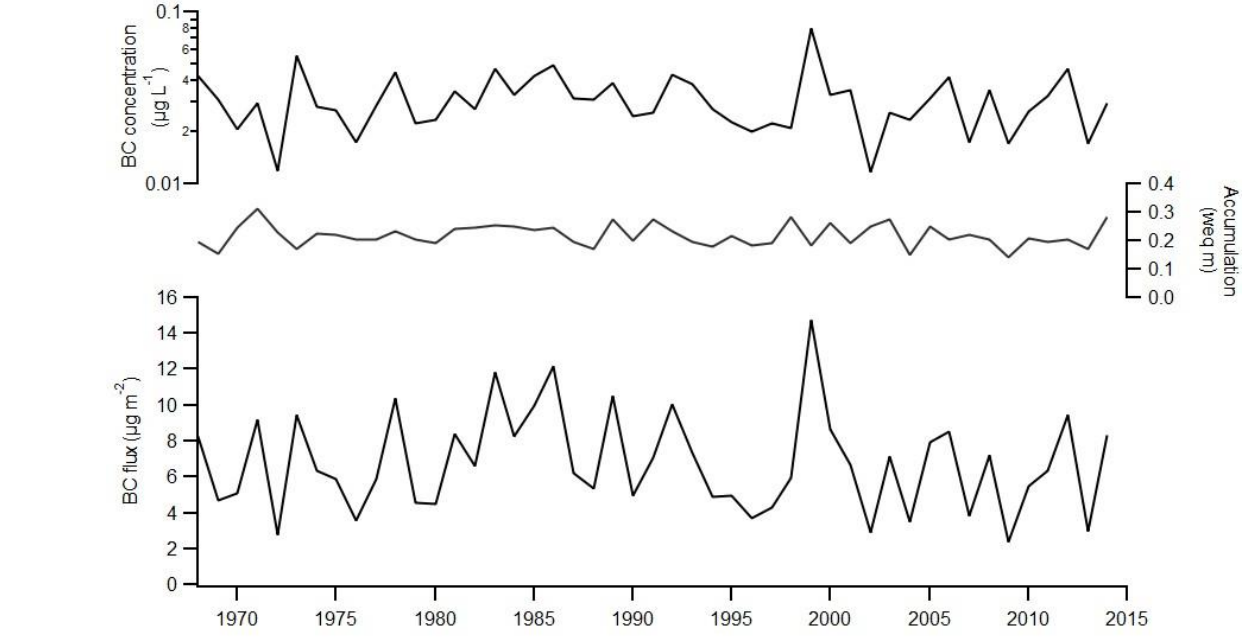

555 **Figure 5. rBC concentrations (y axis logarithmic), accumulation and fluxes for TT07.**

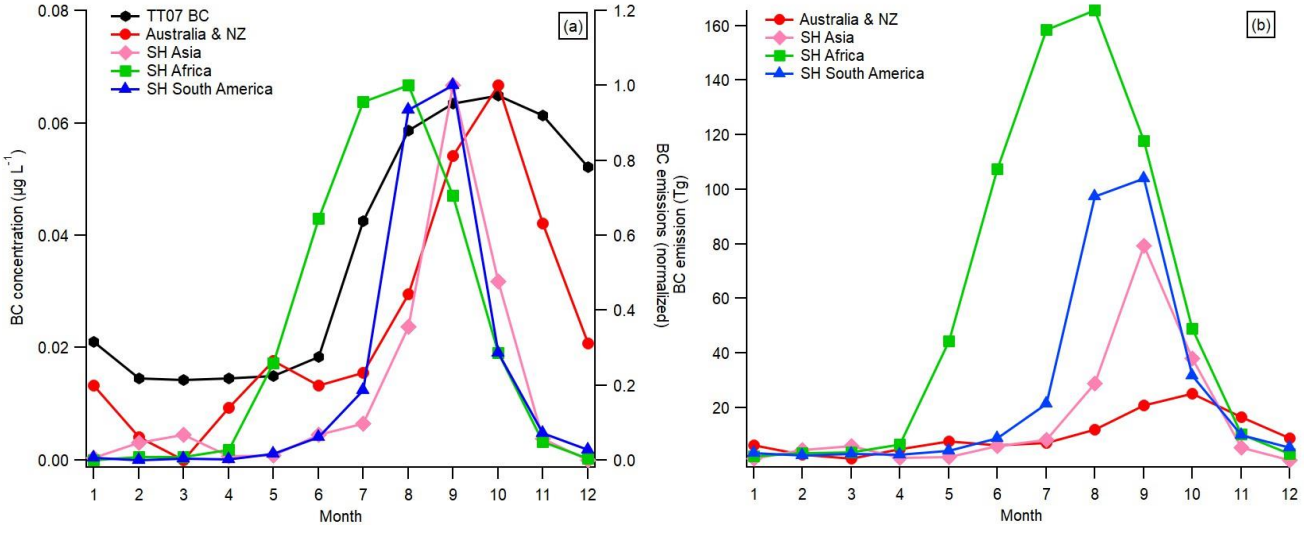

Figure 6(a). TT07 rBC (monthly averages, 1968-2014) and BC emissions estimated from GFED4s for the four SH regions (normalized, 1997-2014). (b) Absolute BC emissions estimated from GFED4s for the SH.

https://doi.org/10.5194/tc-2019-207
Preprint. Discussion started: 6 November 2019
© Author(s) 2019. CC BY 4.0 License.

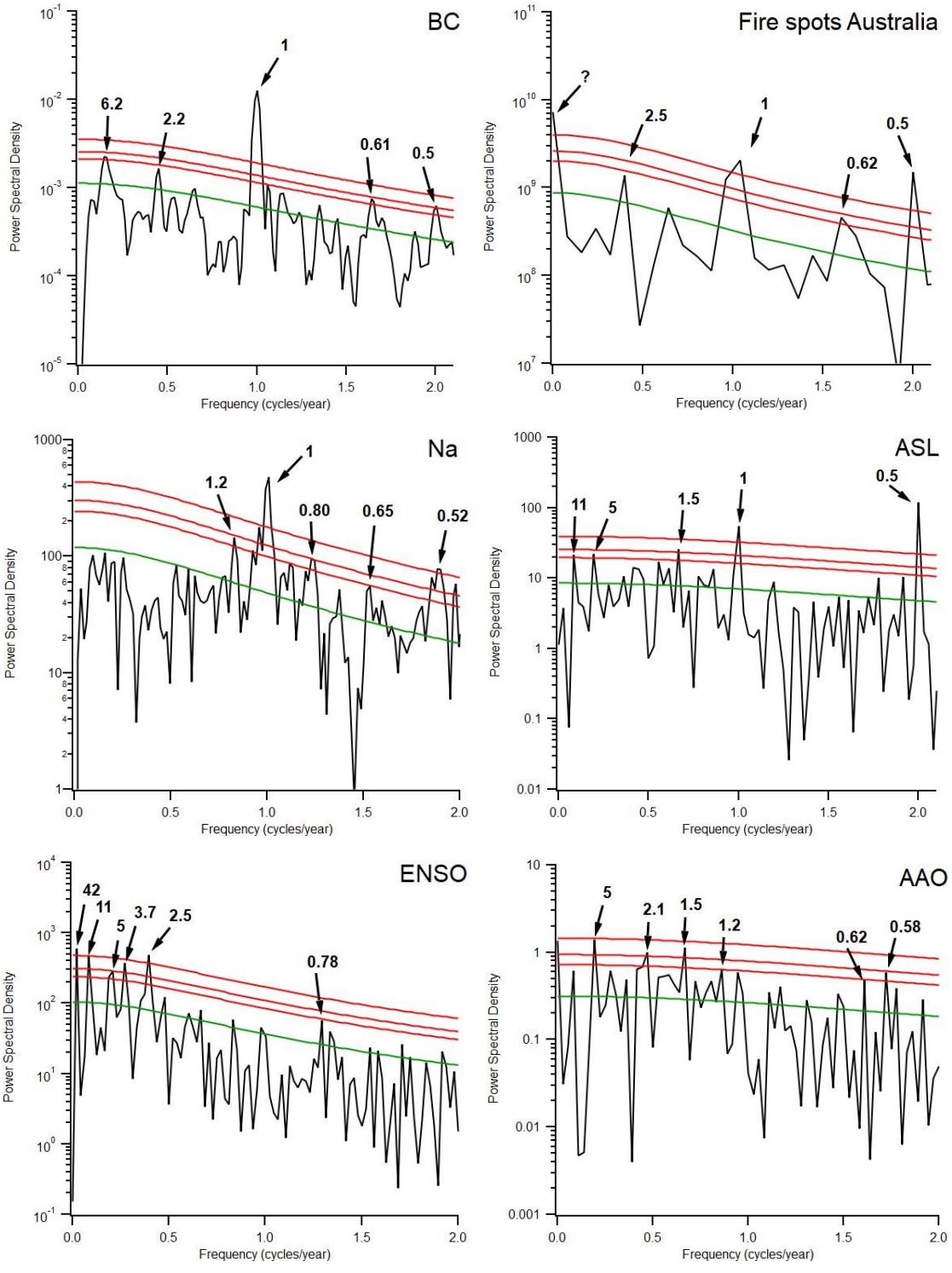

Figure 7. Spectral analysis of the rBC and Na records and comparison with existing datasets (Sentinel Hotspots Australia, ASL, AAO and ENSO indexes). Numbers in bold indicate cycle frequency, in years. Red lines are confidence intervals 99% (top), 95%

https://doi.org/10.5194/tc-2019-207
Preprint. Discussion started: 6 November 2019
© Author(s) 2019. CC BY 4.0 License.

565 **(middle) and 90% (bottom). Green line indicates AR1 red-noise background. The question mark in the Australian fire spots spectrum indicates a longer, unidentified cycle.**

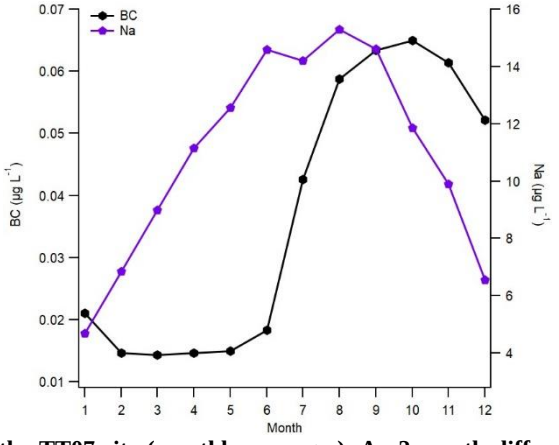

Figure 8. rBC and Na seasonality in the TT07 site (monthly averages). A ~2 month difference is observed between the records, with Na leading rBC.

570 **Table 1. Parameters used to calculate albedo changes in snow for the TT07 site.**

Incident-Flux	Diffuse
Surface spectral distribution	Summit Greenland clear-sky
Snowpack effective grain size	150 µm
Snowpack thickness	20 m
Snowpack density	400 kg/m^3
Visible albedo of underlying surface	0.2
Near-IR albedo of underlying surface	0.4
Uncoated black carbon concentration	Varied, see text
Sulfate-coated black carbon concentration	0 ppb
Dust concentration	0 ppm
Volcanic ash concentration	0 ppm
Experimental particle 1 concentration	0 ppb
MAC scaling factor	1.0

Table 2. Datasets used for the REDFIT spectral analysis.

Dataset	Data points	Range	Observation	Source

https://doi.org/10.5194/tc-2019-207
Preprint. Discussion started: 6 November 2019
© Author(s) 2019. CC BY 4.0 License.

rBC	860	January 1969 December 2014	raw data[a]	TT07 core
Na	813	January 1969 December 2014	raw data[a]	TT07 core
ENSO[b]	576	January 1967 December 2014	Monthly data	Bureau of Meteorology, Australia[c]
AAO	432	January 1979 December 2014	Monthly data	NOAA[d]
ASL	432	January 1979 December 2014	Monthly data	BAS, Hosking *et al.* (2016)[e]
GFED4s	216	January 1997 December 2014	Monthly data	Global Fire Emission Database
Sentinel Hotspots	150	August 2002 December 2014	Monthly data	Geoscience Australia
Programa Queimadas	200	May 1998 December 2014	Monthly data	INPE

[a] Not resampled, only dated by year and separated by dry/wet season.
[b] Here we use the Southern Oscillation index – SOI as the ENSO indicator.
[c] http://www.bom.gov.au/climate/current/soihtm1.shtml
[d] https://www.cpc.ncep.noaa.gov/products/precip/CWlink/
[e] https://legacy.bas.ac.uk/data/absl/

Table 3. Main results from the core rBC analysis. All values in µg L-1, except fluxes, that are in µg m^{-2} yr^{-1}. Geomean = geometric mean and 1σ* = multiplicative standard deviation, representing 68.3% of the variability (Bisiaux et al., 2012b; Limpert et al., 2001)**.**

Total samples	860
Annual geomean	0.03
1σ* interval	0.020 / 0.041
Lowest/highest	0.012 / 0.080
Dry season geomean	0.057
1σ* interval	0.031 to 0.105
Lowest/highest	0.005 / 0.332
Wet season geomean	0.015
1σ* interval	0.009 to 0.027
Lowest/highest	0.001 / 0.053
rBC flux geomean	6.24
Lowest/highest	2.67 / 14.61

Table 4. Coordinates, elevation, period covered and rBC information for this study and previous studies in Antarctica with time overlap with this study. We show only studies that used the SP2 in snow/ice to have a direct comparison between them.

https://doi.org/10.5194/tc-2019-207
Preprint. Discussion started: 6 November 2019
© Author(s) 2019. CC BY 4.0 License.

The Cryosphere Discussions
Open Access
EGU

		Location in Antarctica	Lat/ Long	Elev. (m)	Period Covered	Annual rBC conc. (μg L^{-1})	rBC conc. range (2σ)[a]	Annual accum. (w eq m)	Annual rBC fluxes (μg m^{-2})	rBC flux range (2σ)[a]
This study	TT07	West	82°40'S 89°55'W	2122	1968-2015	0.03	0.01 to 0.07	0.23	6.13	2.8 to 14.4
Bisiaux *et al.*, 2012b	WAIS	West	79°46'S 112°08'W	1766	1963-2001[b]	0.08	0.05 to 0.12	0.2	16	9.8 to 24.4
	Law Dome	East	66°73'S 112°83'E	1390	1963-2001[b]	0.07	0.04 to 0.15	0.15	13.5	7.3 to 30.6
Bisiaux *et al.*, 2012b	NUS07-1	East	73°43'S 07°59'E	3174	1963-2006[b]	0.14	0.08 to 0.27	0.05	7.8	4.0 to 15.8
	NUS07-2		76°04'S 22°28'E	3582	1963-1993[b]	0.14	0.08 to 0.24	0.03	3.9	2.4 to 7.3
	NUS07-5		78°39'S 35°38'E	3619	1963-1989[b]	0.18	0.14 to 0.24	0.02	3.62	2.6 to 5.2
	NUS07-7		82°49'S 54°53'E	3725	1963-2008[b]	0.19	0.13 to 0.29	0.02	5	3.1 to 8.0
	NUS08-4		82°49'S 18°54'E	2552	1963-2004[b]	0.15	0.08 to 0.26	0.04	5.4	2.7 to 10.0
	NUS08-5		82°38'S 17°52'E	2544	1963-1993[b]	0.12	0.08 to 0.20	0.04	4.5	2.7 to 8.0
Casey *et al.*, 2017	Clean air sector	South Pole	90°S	2835	Surface snow (2014-2015)	0.24[c]	-	-	-	-
	Upwind of generator					0.48[c]	-	-	-	-
Khan *et al.*, 2018	Snowpit 1 m deep	McMurdo Dry Valleys	77°31'S 163°E	-	2006-2013	0.35[c]	-	-	-	-

[a] Multiplicative standard deviation representing 95.5% of the interval of confidence
[b] Core goes back to ~1800, we present only from 1963 on to have time overlap between these and this study.
[c] Not annual.

585

Table 5. Albedo changes due to rBC concentrations in TT07 site (from SNICAR-online).

Concentration (μg L^{-1})	Reference	Albedo variation (relative to clean snow)
0.015	Wet season geomean	0
0.057	Dry season geomean	-0.41%
0.105	Highest seasonal geomean	-0.48%